

RESEARCH ARTICLE

# Dual Role of a Biosynthetic Enzyme, CysK, in Contact Dependent Growth Inhibition in Bacteria

Soni Kaundal, Manju Uttam, Krishan Gopal Thakur\*

Structural Biology Laboratory, G. N. Ramachandran Protein Centre, Council of Scientific and Industrial Research-Institute of Microbial Technology, Chandigarh, India

\* [krishang@imtech.res.in](mailto:krishang@imtech.res.in)



**OPEN ACCESS**

**Citation:** Kaundal S, Uttam M, Thakur KG (2016) Dual Role of a Biosynthetic Enzyme, CysK, in Contact Dependent Growth Inhibition in Bacteria. PLoS ONE 11(7): e0159844. doi:10.1371/journal.pone.0159844

**Editor:** Hang Hubert Yin, University of Colorado Boulder, UNITED STATES

**Received:** January 21, 2016

**Accepted:** July 8, 2016

**Published:** July 26, 2016

**Copyright:** © 2016 Kaundal et al. This is an open access article distributed under the terms of the [Creative Commons Attribution License](https://creativecommons.org/licenses/by/4.0/), which permits unrestricted use, distribution, and reproduction in any medium, provided the original author and source are credited.

**Data Availability Statement:** All relevant data are within the paper.

**Funding:** This work was supported by Council of Scientific and Industrial Research, India grant no. OLP0077 to KGT. SK is a senior research fellow, University Grants Commission, India.

**Competing Interests:** The authors have declared that no competing interests exist.

## Abstract

Contact dependent growth inhibition (CDI) is the phenomenon where CDI<sup>+</sup> bacterial strain (inhibitor) inhibits the growth of CDI<sup>-</sup> strain (target) by direct cell to cell contact. CDI is mediated by *cdiBAI* gene cluster where CdiB facilitates the export of CdiA, an exotoxin, on the cell surface and CdiI acts as an immunity protein to protect CDI<sup>+</sup> cells from autoinhibition. CdiA-CT, the C-terminal region of the toxin CdiA, from uropathogenic *Escherichia coli* strain 536 (UPEC536) is a latent tRNase that requires binding of a biosynthetic enzyme CysK (O-acetylserine sulfhydrylase) for activation in the target cells. CdiA-CT can also interact simultaneously with CysK and immunity protein, CdiI, to form a ternary complex in UPEC536. But the role of CysK in the ternary complex is not clear. We studied the hydrodynamic, thermodynamic and kinetic parameters of binary and ternary complexes using AUC, ITC and SPR respectively, to investigate the role of CysK in UPEC536. We report that CdiA-CT binds CdiI and CysK with nanomolar range affinity. We further report that binding of CysK to CdiA-CT improves its affinity towards CdiI by ~40 fold resulting in the formation of a more stable complex with over ~130 fold decrease in dissociation rate. Thermal melting experiments also suggest the role of CysK in stabilizing CdiA-CT/CdiI complex as T<sub>m</sub> of the binary complex shifts ~10°C upon binding CysK. Hence, CysK acts a modulator of CdiA-CT/CdiI interactions by stabilizing CdiA-CT/CdiI complex and may play a crucial role in preventing autoinhibition in UPEC536. This study reports a new moonlighting function of a biosynthetic enzyme, CysK, as a modulator of toxin/immunity interactions in UPEC536 inhibitor cells.

## Introduction

In most of the natural environments, microbes live in communities and adopt several survival strategies to compete or cooperate for limited resources [1]. In these microbial communities, bacteria have developed complex mechanisms to communicate with each other, either by secreting and sensing small chemical messenger molecules which involves phenomenon known as quorum sensing or by direct cell to cell contact. These bacterial communication

systems help in coordinating multicellular behaviour like bioluminescence, biofilm formation, virulence, production of nanowire etc. and might also participate in discriminating 'self' or kin from 'non-self' or non-kin strains [2–6]. Direct cell to cell contact is probably a strategy by which bacteria can modulate the growth and behaviour of both siblings and competitors in close contact.

In 2005, Low and his co-workers coined a term “Contact Dependent growth Inhibition (CDI)” to describe a phenomenon where inhibitor cells require direct cell to cell contact to inhibit the growth of the target cells [7] (Fig 1). They further showed that CDI is mediated by *cdiBAI* gene cluster. CdiA and CdiB are components of two-partner secretion (TPS) system [8,9]. CdiB is a predicted  $\beta$ -barrel protein that facilitates export of CdiA across the outer membrane. CdiA is a large exotoxin, ranging from 180–600 kDa, consisting of long filamentous hemagglutinin repeats and a toxic tip [10,11]. Multiple sequence analyses of the N-terminal region of CdiA from different species shows high sequence similarity, however, the C-terminal 200–300 residues, CdiA-CT, are highly divergent and predicted to have a wide range of catalytic and non-catalytic toxic activities [9,11]. CdiA is predicted to form a long filament from the surface of the inhibitor cell (CDI<sup>+</sup>) to bind the receptor on the target bacteria (CDI<sup>-</sup>) [9]. Since CdiA/CdiB shares sequence conservation with TPS systems so it is likely that CdiA protein folds outside the cell, as observed in TpsA protein [9,12]. But inhibitor cells face potential threat from re-entry of CdiA-CT toxin. These cells are prevented from autoinhibition due to the presence of an immunity protein, CdiI [7]. CdiI binds and neutralizes only the cognate CdiA-CT but not the heterologous ones [11]. These immunity proteins allow genetic counterparts of inhibitor cells to proliferate and outnumber their competitors [7]. Polymorphic nature of toxic tips also suggests that different bacteria may have different strategies to kill competitors or avoid the toxin neutralization from immunity proteins of the target cells [11,13]. Bioinformatics analyses suggest that CDI systems are widespread and are present in many plant, animal and human pathogens as well [5,11,13–15]. The CDI systems have so far been discovered in gram-negative bacteria and only acts upon closely related strains [7,16]. CDI systems have also been implicated in shaping biofilm structures to prevent non-self bacteria from entering the

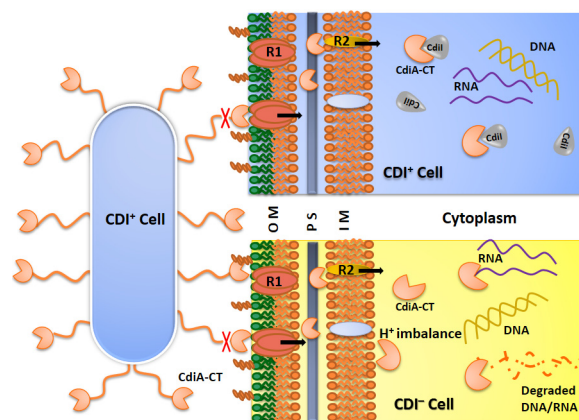


**Fig 1. Schematic representation of mechanism of Contact Dependent Growth Inhibition in bacteria.** CDI<sup>+</sup> inhibitor cell expresses CdiA toxin on the cell surface. Upon coming in contact with receptor(s) present on the outer membrane of the cell, CdiA is cleaved and only toxic tip, CdiA-CT, enters the cell to reach molecular targets in the cytoplasm. CDI<sup>+</sup> cells express CdiI which bind and neutralize cognate CdiA-CT to prevent autoinhibition. In CDI<sup>-</sup> cells CdiA-CT toxins act on different molecular targets like DNA, RNA, membrane etc. and causes growth arrest. This model is based on the published literature on CDI system from *E. coli* EC93 [7,9,20]. Abbreviations used: OM, Outer Membrane; PS, Periplasmic Space; IM, Inner Membrane; R1, Receptor 1; R2, Receptor 2

doi:10.1371/journal.pone.0159844.g001

community [17,18]. In our study, we have investigated CDI system from a UPEC536, which causes recurrent urinary tract infection [19].

Recent studies suggest that CDI toxins exploit multiple target proteins to gain access to the target molecules localized in cytoplasm or membrane [9,21,22]. UPEC536 CDI system is more complex as compared to other CDI systems, as, besides the selection of target cell at the level of receptor-mediated uptake of a toxin, an additional step of selection was observed in the form of a biosynthetic enzyme, CysK (O-acetylserine sulphydrylase). CysK acts as a “permissive factor” that activates the otherwise inactive CdiA-CT and no significant growth inhibition was observed in the  $\Delta$ CysK target cells [23]. CdiA-CT was shown to have tRNase activity in *in vivo* but purified toxin failed to show any activity in *in vitro* conditions. This led to the discovery of a host factor, CysK as an activator of tRNase activity of the CdiA-CT. Purified CysK activates CdiA-CT tRNase while CdiI (cognate immunity protein of CdiA-CT) is sufficient to block the resulting nuclease activity. Pull down assays have demonstrated that CdiA-CT forms a stable ternary complex with CysK and CdiI and both interacting partners bind non-overlapping sites on CdiA-CT. The C-terminal isoleucine residue of CdiA-CT is critical for CdiA-CT/CysK interactions as CdiA-CT<sup>( $\Delta$ I3242)</sup> mutant is not able to bind CysK and lacks tRNase activity *in vitro* [23]. Given the fact that CdiA-CT, CdiI and CysK form a ternary complex within the inhibitor (CDI<sup>+</sup>) cells, the role of CysK and the basis of formation of this ternary complex in UPEC536 cells remain to be elucidated.

To address this important intriguing question, we investigated the role of CysK/CdiA-CT interactions in the context of inhibitor cell. We report for the first time the thermodynamic and kinetic parameters, oligomeric states and stoichiometry of proteins and protein-protein complexes involved in the CDI systems. We report a new moonlighting role of CysK in stabilizing CdiA-CT/CdiI immunity complex in UPEC536 and thus preventing autoinhibition. Taken together our findings and past reports, we propose that CysK plays two contrast roles—as a modulator of immunity complex in the inhibitor cells and as a toxin activator in the target cells, in UPEC536 mediated CDI. Our study establishes the significance of CysK in stabilizing inactive ternary complex in UPEC536 cells.

## Materials and Methods

### Cloning of Genes

In our experience, we have observed high toxicity of CdiA-CT toxin in *E. coli* as we could not get the functional gene cloned or expressed even in the presence of immunity protein gene. So, we used active site mutant CdiA-CT<sup>536(H3193A)</sup>, labeled CdiA-CT<sup>(M)</sup>, in our studies. This mutant reportedly lacks nuclease activity and retains gross structural architecture as evident from its tight association with the binding partner, CdiI [24]. Codon optimized synthetic genes *cdiA-CT*<sup>(M)</sup> (Gly 3009-Ile 3242) and full-length *cdiI* were procured from GenScript USA Inc. *cdiA-CT*<sup>(M)</sup>, *cdiI* and *cysK* (amplified from *E. coli* K12 genomic DNA) gene products were cloned between NheI/HindIII, NdeI/XhoI and NcoI/XhoI restriction sites to yield pET28a-*cdiA-CT*<sup>(M)</sup>, pET28a-*cdiI* and pNIC28-Bsa4-*cysK* plasmids, respectively. The sequence of each construct was verified by DNA sequencing. All the recombinant proteins contained N-terminal 6x His-tag to aid purification.

### Purification of Proteins

Plasmid carrying desired gene(s) were transformed in *E. coli* BL21(DE3) cells and plated on LB agar plate having 50  $\mu$ g/mL kanamycin and were incubated overnight at 37°C. Primary culture was prepared by inoculating single colony in 5 ml LB media and incubated overnight with constant shaking at 37°C. Primary culture was inoculated in 500 mL of LB media in shake flask

and cells were induced by adding 0.3 mM IPTG at 0.6 OD<sub>600</sub>. Cells were further incubated at 18°C for overnight with constant shaking at 200 rpm. Cells were harvested by centrifugation at 7000g for 10 min and pellet was re-suspended in lysis buffer (20 mM HEPES pH 7.5, 250 mM NaCl, and a cocktail of protease inhibitors) followed by sonication. The supernatant was collected after centrifugation at 18000g for 45 min. The protein was purified using Co-NTA (Gold Biotechnology, USA) followed by gel filtration using Superdex 200 Increase 10/300 GL column (GE Healthcare) as per the standard protocols recommended by the manufacturers. The desired elution fractions were pooled and concentrated using ultrafiltration centrifugal devices (Pall Corporation). The purity and quality of the protein samples were analysed using SDS-PAGE and mass spectrometry. All the target proteins CdiA-CT<sup>(M)</sup>, CdiI and CysK could be purified using above-mentioned protocol to the purity of >95% as judged by the SDS-PAGE.

### Analytical Size Exclusion Chromatography (SEC)

Oligomeric state of purified proteins was analysed using the high resolution Superdex 200 Increase 10/300 GL column. 0.5 ml of concentrated samples (10, 20 and 30 μM) were loaded on the column which was pre-equilibrated with the running buffer (20 mM HEPES pH 7.5 and 250 mM NaCl). A constant flow rate of 0.5 ml/min was used and UV absorbance was monitored simultaneously at 280 nm, 254 nm and 220 nm at ~ 15°C. Standard calibration curve for the column was prepared using low molecular weight gel filtration calibration kit (GE Healthcare). To study protein-protein complexes, purified proteins were mixed (in varying molar ratios) and incubated at 4°C for 1 h before conducting SEC and analytical ultracentrifugation (AUC) experiments. The elution fractions were analysed using SDS-PAGE.

### Analytical Ultracentrifugation

AUC experiments were performed using Beckman-Coulter XL-A analytical ultracentrifuge equipped with a TiAn50 eight hole rotor to study the oligomeric state and stoichiometry of proteins and protein-protein complexes. Two-channel epon centrepieces (12 mm) and quartz windows were used for sedimentation velocity experiments. Three different concentrations of protein samples (10, 20 and 30 μM in the same buffer as used in the SEC experiments) were run and absorbance scans were recorded at 280 nm at every 3 or 4 min interval at 40,000 rpm at 15°C. Continuous distribution c(s) model was used to fit multiple scans at regular intervals with SEDFIT [25]. The solvent density ( $\rho$ ) and viscosity ( $\eta$ ) were calculated from the chemical composition of different proteins by SEDNTERP [26]. The values presented are the result of three independent experiments and the uncertainties were calculated using standard deviation.

### Isothermal Titration Calorimetry (ITC)

To determine the  $K_D$ , stoichiometry and thermodynamic parameters of binding, ITC experiments were performed at 30°C using MicroCal VP-ITC (GE Healthcare). All the purified proteins were dialyzed against the buffer (20 mM HEPES pH 7.5, 150 mM NaCl), using dialysis membrane of 3500 MWCO. Degassing was performed using MicroCal ThermoVac (GE Healthcare) prior to the experiments. CdiA-CT<sup>(M)</sup> (10 μM; sample cell) was titrated with CdiI (300 μM; syringe), and CdiA-CT<sup>(M)</sup> (20 μM; sample cell) was titrated with CysK (120 μM dimer; syringe) with the constant stirring speed of 307 rpm. The injection volume and reference power were kept 6 μl and 5 μcal/sec respectively. To study the binding of CdiA-CT<sup>(M)</sup>/CysK complex with CdiI, the complex CdiA-CT<sup>(M)</sup>/CysK (5 μM heterotetramer; sample cell) was titrated with CdiI (100 μM; syringe) and for the binding of CdiA-CT<sup>(M)</sup>/CdiI with CysK, the complex CdiA-CT<sup>(M)</sup>/CdiI (30 μM heterodimer; sample cell) was titrated with CysK (150 μM dimer; syringe). One-site binding model was used to analyse CdiA-CT<sup>(M)</sup>/CdiI

interactions. Since CysK is a dimer so based on the published literature, two binding site model was used to analyse protein-protein interactions involving CysK [27,28]. The binding isotherms were fit to determine apparent molar reaction enthalpy ( $\Delta H$ ), apparent entropy ( $\Delta S$ ), dissociation constant ( $K_D$ ) and stoichiometry of binding ( $N$ ). To calculate ligand heat of dilution, experiments were performed under same experimental conditions except protein in the sample cell was replaced with the buffer. In all the calculations ligand heat of dilution was subtracted from the data. The data were analysed using Origin 6.0 software suite.

## Surface Plasmon Resonance (SPR)

To measure the kinetics of CdiA-CT<sup>(M)</sup> binding to CdiI and CysK, SPR experiments were performed using Biacore 3000 at 30°C. CdiA-CT<sup>(M)</sup> was diluted to 1  $\mu$ M concentration in 10 mM sodium acetate (pH 5.0) and 723 response units (RU) were immobilized on the surface of the CM5 sensor chip. All experiments were carried out at a continuous flow rate of 20  $\mu$ l/min using filtered and degassed buffer (10 mM HEPES pH 7.5, 150 mM NaCl). The association and dissociation were observed for 300 s and 500 s for each complexes. The dissociation sensograms have been trimmed for better presentation of data. The analyte, CdiI was injected in a concentration gradient from 5 nM to 40 nM. The surface was regenerated by injecting 5  $\mu$ l of 20 mM NaOH at flow rate of 5  $\mu$ l/min. All the experiments were repeated at least three times at each concentration. The sensograms were analysed using BIA evaluation software 3.0 using a 1:1 Langmuir binding model of interaction. Whereas the analyte, CysK was injected in a concentration gradient from 0.4  $\mu$ M to 6.4  $\mu$ M (dimer concentration) followed by regeneration protocol as mentioned above. To study the kinetics of CdiA-CT<sup>(M)</sup>/CysK complex with CdiI, in first step 0.6  $\mu$ M CysK (dimer) was passed over CdiA-CT<sup>(M)</sup> to allow the formation of CdiA-CT<sup>(M)</sup>/CysK complex and then CdiI was injected in a concentration gradient from 2.5 nM to 40 nM followed by regeneration protocol as mentioned above. These experiments were conducted on a separate CM5 sensor chip where 760 RU of CdiA-CT<sup>(M)</sup> were immobilized. The obtained sensograms were analysed using BIAevaluation software 3.0 using a local fitting for separate  $k_a/k_d$  binding model of interaction.

## Thermal Stability Assay

To determine the effect of CysK binding on the thermal stability of the CdiA-CT<sup>(M)</sup>/CdiI complex we performed thermal melting assay using JascoJ-815 CD instrument. Experiments were performed using protein samples in concentration range of 3 to 5  $\mu$ M dissolved in buffer containing 10 mM sodium phosphate, pH 7.4. Protein unfolding was observed by following the change in ellipticity at 220 nm wavelength as a function of temperature. The temperature was scanned from 25–95°C at a ramp rate of 1°C/min. The data were analysed using Origin 6.0 software.

## Results

### CdiA-CT<sup>(M)</sup> and CdiI are monomer in solution and forms 1:1 stoichiometric complex

To determine the oligomeric state of CdiA-CT<sup>(M)</sup> (26.9 kDa) and CdiI (16.8 kDa), a combination of SEC and AUC were used. SEC experiments were performed using Superdex 200 Increase 10/300 GL column as described in the materials and methods section. Purified CdiA-CT<sup>(M)</sup> eluted as a major peak at  $14.3 \pm 0.04$  mL which corresponds to a molecular weight of approximately ~51 kDa suggesting the apparent dimeric state of CdiA-CT<sup>(M)</sup> in solution (Fig 2A). On the contrary, AUC data shows that major population of CdiA-CT<sup>(M)</sup> exists as a monomer and a minor population (~5–10%) as a higher order oligomer i.e. tetramer (Fig 2B;

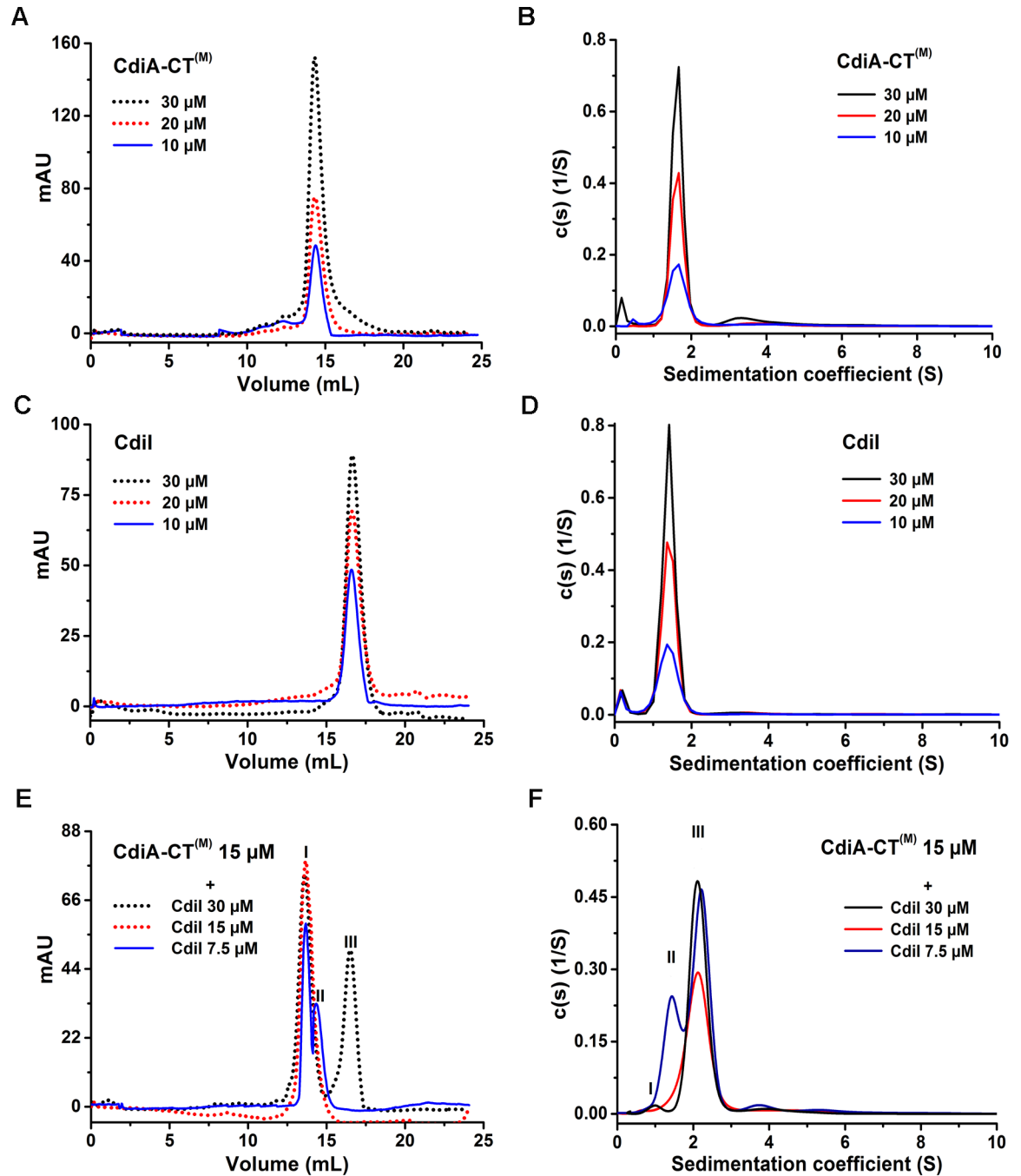


**Fig. 1**

**Fig 2. SEC and AUC analyses of the CdiA-CT<sup>(M)</sup>, CdiI and CdiA-CT<sup>(M)</sup>/CdiI complex.** Sedimentation coefficient distribution  $c(s)$  are shown in the right panels and SEC profiles for the same samples are shown in the left panels. (A) and (B) Single predominant peak of CdiA-CT<sup>(M)</sup> in SEC and AUC data respectively, suggest monodisperse samples. (C) and (D) CdiI also shows a predominant monomeric peak in both SEC and AUC respectively and no significant concentration dependent oligomerization was observed. (E) SEC analysis of CdiA-CT<sup>(M)</sup>/CdiI complex. Peaks I, II and III corresponds to CdiA-CT<sup>(M)</sup>/CdiI complex, CdiA-CT<sup>(M)</sup> and CdiI respectively. Single major peak was observed when CdiA-CT<sup>(M)</sup> and CdiI were mixed in 1:1 molar ratio. (F) AUC data suggests 1:1 stoichiometric complex of CdiA-CT<sup>(M)</sup>/CdiI (peak III). Under sub-stoichiometric conditions peak I correspond to excess CdiI and peak II corresponds to excess CdiA-CT<sup>(M)</sup>.

doi:10.1371/journal.pone.0159844.g002

**Table 1. Comparison of SEC and AUC data of proteins and protein-protein complexes indicating the oligomeric states and the binding stoichiometry.** MW<sub>obs</sub> and MW<sub>cal</sub> are the observed and calculated molecular weights of the sample in kDa, respectively. The percentage population of the complexes mentioned in the parentheses corresponds to the samples where complexes were prepared by mixing equimolar ratio of the protein components.

Sample	MW <sub>cal</sub> (kDa)	SEC		AUC			
		MW <sub>obs</sub> (kDa)	Oligomeric State/ Stoichiometry	MW <sub>obs</sub> (kDa) (% age)	Oligomeric State/ Stoichiometry	S <sub>w</sub> (S)	Frictional ratio
CdiA-CT <sup>(M)</sup>	26.9	~51	Apparent Dimer	26.6 ± 0.07 (84%)	Monomer	1.7 ± 0.01	1.8 ± 0.01
CdiI	16.8	~20	Monomer	16.6 ± 0.02 (90%)	Monomer	1.5 ± 0.01	1.5 ± 0.02
CdiA-CT <sup>(M)</sup> /CdiI	43.7	~67	Heterodimer	41.2 ± 0.12 (70%)	Heterodimer	2.2 ± 0.13	1.89 ± 0.04
CysK	36.7	~70	Homodimer	73.7 ± 0.19 (84%)	Homodimer	4.3 ± 0.06	1.46 ± 0.01
CysK/CdiA-CT <sup>(M)</sup>	63.6	~230	Heterotetramer	126 ± 0.92 (80%)	Heterotetramer	4.1 ± 0.10	2.0 ± 0.02
CysK/CdiA-CT <sup>(M)</sup> / CdiI	80.4	~239	Heterohexamer	157.6 ± 0.52 (77%)	Heterohexamer	5.1 ± 0.14	1.90 ± 0.01

doi:10.1371/journal.pone.0159844.t001

Table 1). The population of this tetramer increases with increasing concentration of the protein. CdiA-CT<sup>(M)</sup> is an elongated molecule as suggested by high frictional ratio observed in the AUC experiment. This elongated shape could explain the apparent dimeric state of CdiA-CT<sup>(M)</sup> observed in the SEC experiments.

CdiI elutes at 16.6 ± 0.02 mL in SEC experiments which corresponds to ~20 kDa molecular weight, thus, suggesting monomeric state of CdiI in solution (Fig 2C). AUC data analysis also shows CdiI exists as a monomer in solution which is in agreement with SEC data (Fig 2D; Table 1).

To study the stoichiometry of CdiA-CT<sup>(M)</sup>/CdiI complex, the former was titrated with varying concentrations of the latter. When equal molar ratio of proteins were mixed, a single peak, corresponding to molecular weight of ~67 kDa, was observed in SEC, suggesting CdiA-CT<sup>(M)</sup>/CdiI forms a 2:1 complex (peak I, Fig 2E). Same complex, when analysed using AUC shows major population of molecular weight of 41.2 ± 0.12 kDa suggesting 1:1 stoichiometric heterodimer of CdiA-CT<sup>(M)</sup>/CdiI (peak III, Fig 2F; Table 1). To summarize both CdiA-CT<sup>(M)</sup> and CdiI exist as a monomer in solution and forms a 1:1 stoichiometric complex. So, like CdiA-CT<sup>(M)</sup> the elongated nature of the complex (frictional ratio 1.89, Table 1) migrates slowly during SEC experiment suggesting apparently higher molecular weight.

### CdiA-CT<sup>(M)</sup> forms a 2:2 stoichiometric complex with CysK

We performed SEC and AUC experiments to study the oligomeric state of CysK and its binding stoichiometry with CdiA-CT<sup>(M)</sup>. Purified CysK (36.7 kDa) elutes as a single peak at around 13.6 ± 0.06 mL which corresponds to molecular weight of ~70 kDa thus suggesting that CysK exists as a dimer in solution (Fig 3A). AUC data also confirms dimeric state of CysK with the observed molecular weight of 73.7 ± 0.19 kDa (Fig 3B; Table 1). When 7.5 μM of CysK dimer was mixed with 15 μM of CdiA-CT<sup>(M)</sup> a single peak was observed in SEC experiments suggesting CysK binds CdiA-CT<sup>(M)</sup> with 2:2 stoichiometry. The complex elutes as a major peak at 10.7 ± 0.1 mL corresponding to molecular weight of ~230 kDa which is significantly higher than the expected molecular weight for this complex (Fig 3C). AUC data reveals that CdiA-CT<sup>(M)</sup>/CysK associate to form a complex with molecular weight of 126.0 ± 0.92 kDa (~80% population) which matches with the expected molecular weight of 2:2 complex, suggesting CdiA-CT<sup>(M)</sup>/CysK forms a 2:2 stoichiometric complex (Fig 3D; Table 1).

### CysK/CdiA-CT<sup>(M)</sup>/CdiI forms a heterohexamer in 2:2:2 stoichiometry

CysK, CdiA-CT<sup>(M)</sup> and CdiI form a stable ternary complex [23]. The oligomeric state and stoichiometry of this ternary complex are not known. So, we experimentally determined the

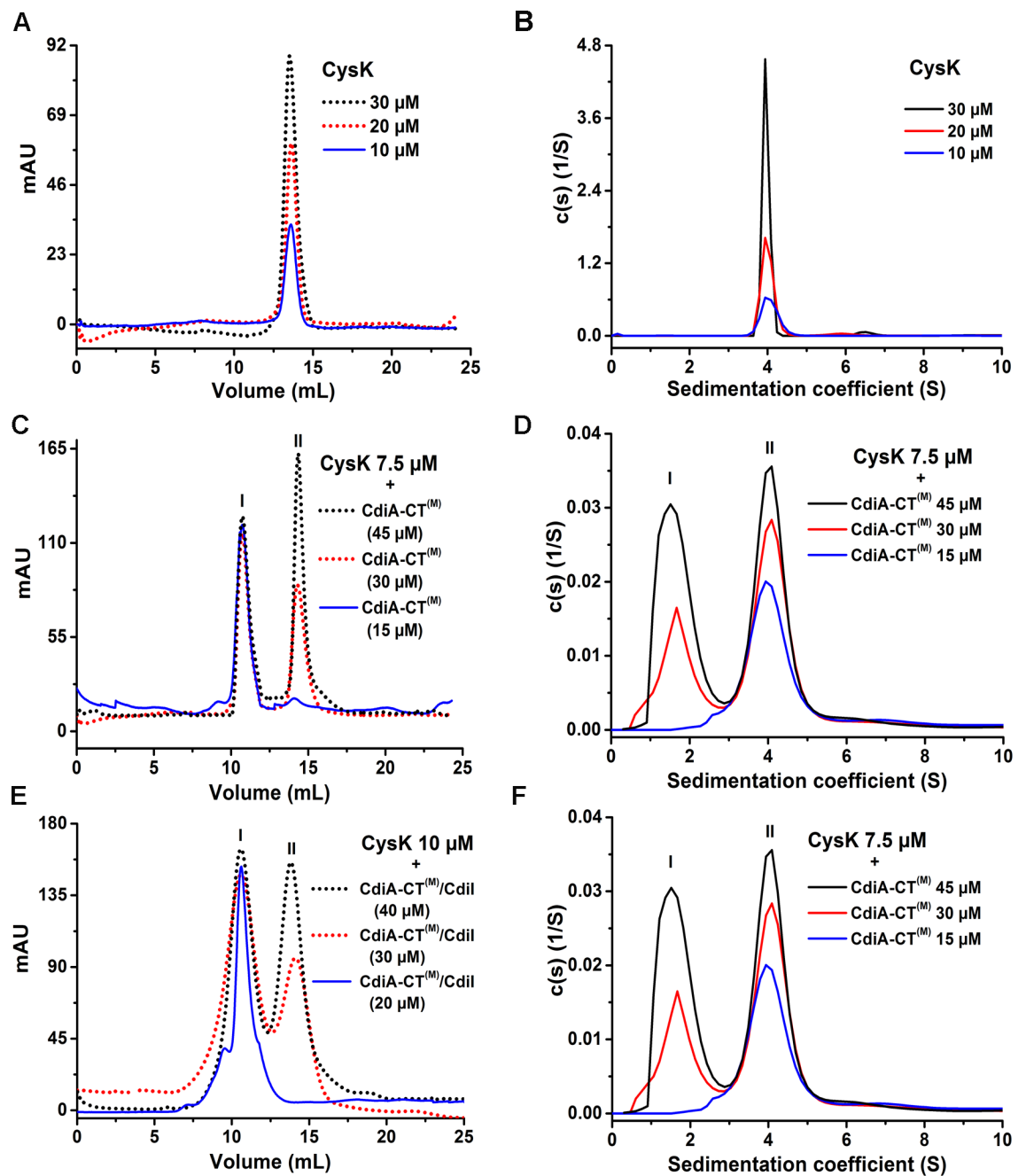


**Fig 3. SEC and AUC analyses of the CysK, CdiA-CT<sup>(M)</sup>/CysK and CdiA-CT<sup>(M)</sup>/CdiI/CysK complexes.** (A) and (B) Both SEC and AUC data suggests dimeric state of CysK. (C) CdiA-CT<sup>(M)</sup>/CysK complex elutes as a single peak when mixed 0.5:1 molar of CysK dimer:CdiA-CT<sup>(M)</sup>. Peak I, CdiA-CT<sup>(M)</sup>/CysK complex; peak II, excess CdiA-CT<sup>(M)</sup>. (D) AUC analysis suggests 2:2 stoichiometric complex of CdiA-CT<sup>(M)</sup>/CysK. Peaks I and II corresponds to CdiA-CT<sup>(M)</sup> and CdiA-CT<sup>(M)</sup>/CysK complex, respectively. (E) The stoichiometric homogenous ternary complex is formed when preformed CdiA-CT<sup>(M)</sup>/CdiI complex is mixed with dimeric CysK in 1:0.5 molar ratio. Peak I, CdiA-CT<sup>(M)</sup>/CdiI/CysK complex; peak II, excess CdiA-CT<sup>(M)</sup>/CdiI complex. (F) CdiA-CT<sup>(M)</sup>/CdiI/CysK forms 2:2:2 stoichiometric complex as suggested by AUC. Peak I, CdiA-CT<sup>(M)</sup>/CdiI complex; peak II CdiA-CT<sup>(M)</sup>/CdiI/CysK ternary complex. In all the above experiments dimeric CysK concentration is used.

doi:10.1371/journal.pone.0159844.g003



oligomeric state of the ternary complex. Ternary complex elutes as a major peak at  $10.6 \pm 0.2$  ml in SEC corresponding to molecular weight of  $\sim 239$  kDa (Fig 3E). This single peak of ternary complex was observed when CysK dimer:CdiA-CT<sup>(M)</sup>/CdiI were mixed in 1:2:2 ratio. AUC data analysis revealed molecular weight of  $157.6 \pm 0.52$  kDa complex which matches well with the expected molecular weight of 160 kDa corresponding to heterohexamer of the CysK/CdiA-CT<sup>(M)</sup>/CdiI complex in 2:2:2 stoichiometry (Fig 3F). High frictional ratio suggests the elongated shape of the ternary complex and possible reason for eluting early in SEC experiments.

### CdiA-CT<sup>(M)</sup> binds CdiI with nanomolar affinity

CDI<sup>+</sup> inhibitory cells are protected from autoinhibition by the presence of an immunity protein (CdiI) which physically interacts with the cognate toxin (CdiA-CT) [7]. To best of our knowledge, there is no study where thermodynamic and kinetic parameters of the toxin/immunity protein interactions involved in CDI systems have been reported. Though antitoxin perform diverse functions [29] they share one common function with immunity protein i.e. both neutralize/inactivate cognate toxin [7,11]. TA systems are produced within cells in response to different stress conditions and regulate gene expression CDI toxins are exotoxins and play an important role in competition. Since there are no reports of kinetic parameters of CDI systems so we compared our results with the bacterial toxin/antitoxin systems. So, in order to characterize the toxin/immunity protein interactions involved in CDI we carried out ITC and SPR experiments. The ITC data suggests 1:1 stoichiometry of binding with  $K_D$  value of  $26.4 \pm 2.1$  nM (Fig 4A) whereas SPR data suggest  $K_D$  value of  $12.8 \pm 1$  nM (Fig 4B) for CdiA-CT<sup>(M)</sup>/CdiI binding at 30°C.  $K_D$  values estimated by the two different techniques are in close agreement. The stoichiometry of 1:1 as estimated from ITC data is in agreement with AUC data. This observed  $K_D$  value for CdiA-CT<sup>(M)</sup>/CdiI is significantly higher as compared to other reported toxin/antitoxin systems including RelB/RelE ( $K_D$ : 0.33nM) [30], SpoII SA/ SpoII SB ( $K_D$ : 0.46 nM) [31], BrnT/BrnA ( $K_D$ : 0.67 nM) [32]. All these reported  $K_D$  values were measured using SPR. The thermodynamic data suggest a negative or favorable binding enthalpy ( $\Delta H$ :  $-2.9 \times 10^4 \pm 115.9$  cal/mol) and unfavorable entropy factor ( $\Delta S$ :  $-60.3$  cal/mol/K) indicating a major role of hydrogen bonding and unfavorable conformational rearrangements in this binding event (Fig 4A; Table 2). SPR data analysis suggested high  $k_{on}$ :  $5.1 \times 10^6$  M<sup>-1</sup>s<sup>-1</sup> and unexpectedly high  $k_{off}$ :  $6.5 \times 10^{-2}$  s<sup>-1</sup> for this complex (Fig 4B). The  $k_{off}$  for CdiA-CT<sup>(M)</sup>/CdiI is significantly higher as compared to the other reported toxin/antitoxin systems including RelB/RelE ( $k_{off}$ :  $1.66 \times 10^{-4}$  s<sup>-1</sup>) [30], SpoII SA/SpoII SB ( $k_{off}$ :  $9.1 \times 10^{-4}$  s<sup>-1</sup>) [31], BrnT/BrnA ( $k_{off}$ :  $1.63 \times 10^{-4}$  s<sup>-1</sup>) [32]. Thus, it is evident that the lower  $K_D$  of CdiA-CT<sup>(M)</sup>/CdiI complex is a consequence of significantly higher  $k_{off}$ . On the basis of the kinetic data we speculate that as the toxin enters the CDI<sup>+</sup> inhibitory cell, CdiI binds CdiA-CT quite rapidly but also apparently breaks apart swiftly as indicated by high  $k_{on}$  and  $k_{off}$ .

### CdiA-CT<sup>(M)</sup> and CysK binds with nanomolar affinity

CysK is required for the nuclease activity of CdiA-CT and both the proteins interact physically to form an activated complex [23]. We used ITC and SPR to determine affinity and kinetics of this toxin/activator (CdiA-CT<sup>(M)</sup>/CysK) complex. ITC data suggest that two monomers of CdiA-CT<sup>(M)</sup> bind with one dimer of CysK with  $K_{D1}$  of  $79.3 \pm 8.9$  nM and  $K_{D2}$  of  $89.2 \pm 10.1$  nM suggesting similar affinities for both the binding sites (Fig 4C). Calculated changes in enthalpy ( $\Delta H_{1,2}$ ) and entropy ( $\Delta S_{1,2}$ ) are summarized in Table 2. SPR data also suggests similar high affinity complex with  $K_D$  of  $32 \pm 4$  nM (Fig 4D). The stoichiometry of 2:2 as estimated from the ITC data is in agreement with the AUC data. SPR data analysis suggests slow rates of association ( $k_{on}$ :  $6.2 \times 10^3$  M<sup>-1</sup>s<sup>-1</sup>) and dissociation ( $k_{off}$ :  $1.4 \times 10^{-4}$  s<sup>-1</sup>) as compared to CdiA-CT<sup>(M)</sup>/CdiI binding.

Low dissociation rate is advantageous for the toxin as upon activation enzyme may remain active for longer period consequently causing growth arrest in the target cell.

### CysK/CdiA-CT<sup>(M)</sup> complex binds CdiI with ~40 fold higher affinity as compared to CdiA-CT<sup>(M)</sup>

Both CdiI and CysK can simultaneously bind CdiA-CT and form a ternary complex which reportedly lacks nuclease activity [23]. To understand the possible role of CysK in this ternary

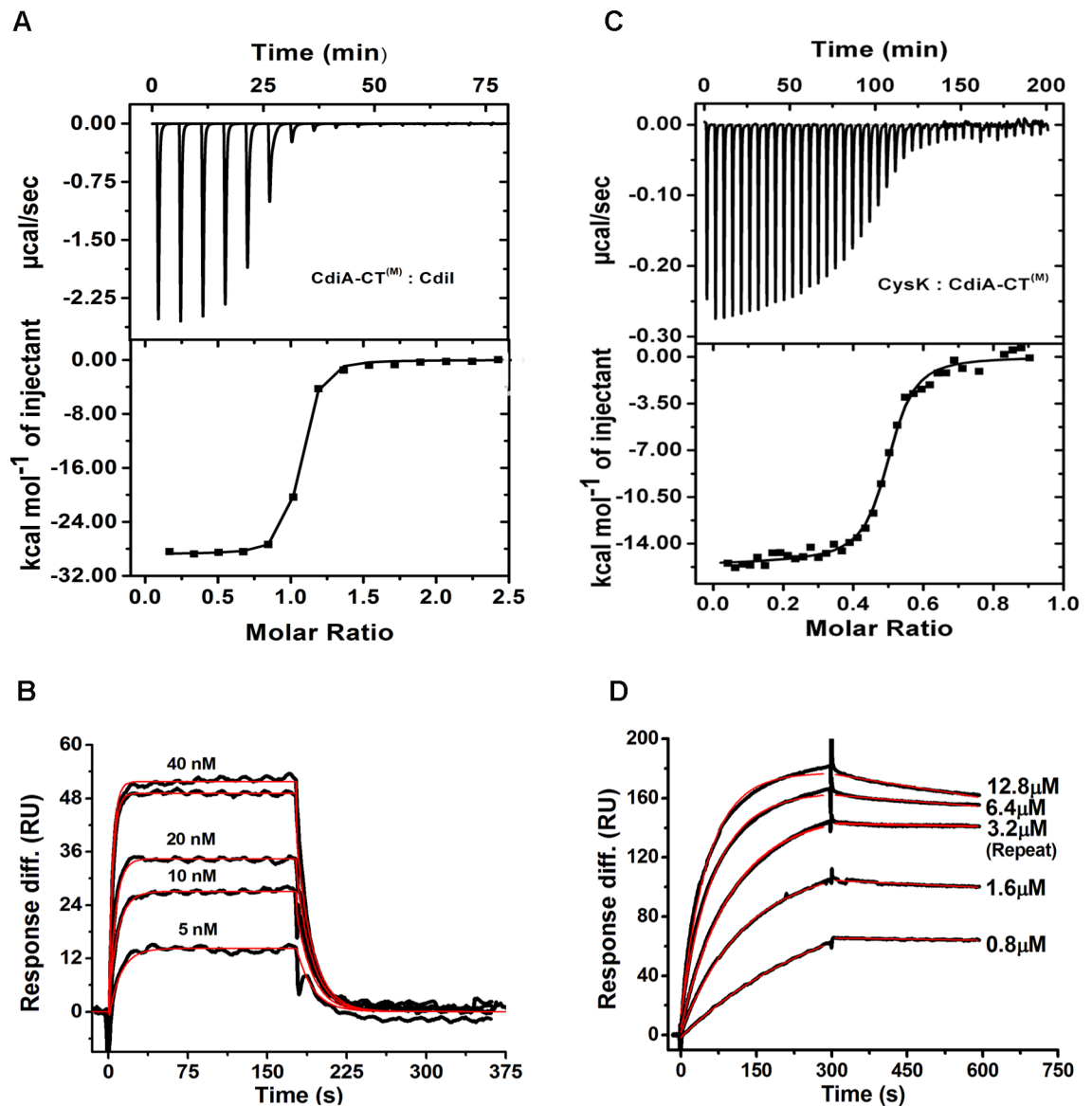


**Fig 4. ITC and SPR data showing kinetics and thermodynamic parameters of protein-protein interactions.** Representative isothermal calorimetric titration curve of (A) CdiA-CT<sup>(M)</sup>/CdiI (C) CdiA-CT<sup>(M)</sup> and CysK. The top panel shows the calorimetric titration and bottom panel shows derived binding isotherm plotted versus the molar ratio of the titrant. The solid line in the lower panel is the best fit to the data using the nonlinear least squares regression algorithm. SPR analysis of binding of (B) CdiA-CT<sup>(M)</sup>/CdiI, (D) CdiA-CT<sup>(M)</sup>/CysK. Both raw sensograms (black lines) and fitted curves (red lines) are shown in the figure. These sensograms are representative of three sets of experiments that we carried out using four to five different concentrations of the analyte. In each figure, one representative sensogram for repeat run is also shown. (CdiA-CT<sup>(M)</sup>/CysK) complex. ITC data suggest that two monomers of CdiA-CT<sup>(M)</sup> bind with one dimer of CysK.

doi:10.1371/journal.pone.0159844.g004

**Table 2. ITC and SPR data showing thermodynamic and kinetic parameters of protein-protein interactions involved in UPEC536 mediated CDI system.** ITC data were fit using one-site binding model for CdiA-CT<sup>(M)</sup>/CdiI and two site binding model for rest of the complexes. The parameters for the second binding site are shown in the parentheses.

Protein samples	ITC				SPR		
	N	$\Delta H$ (cal/mol)	$\Delta S$ (cal/mol/K)	$K_D$ (nM)	$K_D$ (nM)	$k_{on}$ (M <sup>-1</sup> s <sup>-1</sup> )	$k_{off}$ (s <sup>-1</sup> )
CdiA-CT <sup>(M)</sup> + CdiI	0.993	$-2.9 \times 10^4 \pm 115.9$	-60.3	$26.4 \pm 2.1$	$12.8 \pm 1$	$5.1 \times 10^6$	$6.5 \times 10^{-2}$
CdiA-CT <sup>(M)</sup> + CysK	0.494	$-5618 \pm 167.9$ ( $-2.02 \times 10^4 \pm 145.9$ )	14.0 (-34.5)	$79.3 \pm 8.9$ ( $89.2 \pm 10.1$ )	$32 \pm 4$	$6.2 \times 10^3$	$1.4 \times 10^{-4}$
CysK/CdiA-CT <sup>(M)</sup> + CdiI	1.892	$-2.67 \times 10^4 \pm 1.28 \times 10^3$ ( $-2.42 \times 10^4 \pm 1.18 \times 10^3$ )	-46.6 (-38.9)	$1.3 \pm 0.5$ ( $1.1 \pm 0.3$ )	$0.3 \pm 0.08$	$1.5 \times 10^6$	$5.0 \times 10^{-4}$
CdiA-CT <sup>(M)</sup> /CdiI + CysK	0.512	$-1.1 \times 10^4 \pm 157.9$ ( $-2.67 \times 10^4 \pm 267.9$ )	-0.9 (-31.1)	$12.0 \pm 1.9$ ( $13.4 \pm 2.3$ )			

doi:10.1371/journal.pone.0159844.t002

complex in CDI<sup>+</sup> inhibitory cells we investigated CdiA-CT/CdiI interactions by ITC and SPR. To our surprise, ITC data suggested that two CdiI monomer binds preformed CdiA-CT<sup>(M)</sup>/CysK heterotetramer complex with significantly lower  $K_{D1}$ :  $1.3 \pm 0.5$  and  $K_{D2}$ :  $1.1 \pm 0.3$  nM (Fig 5A) which is ~25 fold lower than CdiA-CT<sup>(M)</sup>/CdiI complex. SPR data also suggest ~40 fold lower  $K_D$  ( $0.33 \pm 0.08$  nM) of the ternary complex compared to CdiA-CT<sup>(M)</sup>/CdiI complex (Fig 5B). The thermodynamic parameters of this association are summarized in Table 2. The  $k_{on}$  and  $k_{off}$  of this binding are  $1.5 \times 10^6$  M<sup>-1</sup>s<sup>-1</sup> and  $5.0 \times 10^{-4}$  s<sup>-1</sup>, respectively (Fig 5B). The  $k_{off}$  is ~130 fold lower as compared to that observed for the CdiA-CT<sup>(M)</sup>/CdiI complex. Nonetheless, there is a ~3 fold decrease in the association rate as well. These results indicate that ternary complex is much more stable than CdiA-CT<sup>(M)</sup>/CdiI complex which is majorly the consequence of the decrease in the dissociation rate.

### Binding of CdiI increases the affinity of CysK towards CdiA-CT<sup>(M)</sup>

It is not clear whether ternary complex formation follows a specific binding sequence. So, we studied the affinity of CdiA-CT<sup>(M)</sup>/CdiI complex with CysK. As CdiI has a high dissociation rate (Fig 4) so we could not use SPR for this study. We used ITC where the preformed complex of CdiA-CT<sup>(M)</sup> and CdiI was titrated with CysK. ITC data suggests a high affinity with  $K_{D1}$  of  $12.0 \pm 1.9$  and  $K_{D2}$  of  $13.4 \pm 2.3$  nM (Fig 6) which is ~5 fold lower as compared to that observed for CdiA-CT<sup>(M)</sup>. This suggests that CysK can bind both CdiA-CT<sup>(M)</sup> and CdiA-CT<sup>(M)</sup>/CdiI complex albeit it has a higher affinity for the latter.

### CysK significantly improves thermal stability of CdiA-CT<sup>(M)</sup> and CdiA-CT<sup>(M)</sup>/CdiI

To compare the effect of CysK binding on the thermal stability of CdiA-CT<sup>(M)</sup>/CdiI binary complex, we monitored protein unfolding with increasing temperature using CD. Thermal melting experiments suggest that CdiA-CT<sup>(M)</sup>/CdiI complex exhibit two state melting curve with melting temperature ( $T_m$ ) of  $58.9 \pm 0.2^\circ\text{C}$ . The ternary complex also exhibits two state melting curve showing cooperative unfolding and having  $T_m$  of  $69.0 \pm 0.2^\circ\text{C}$  which is ~10°C higher than the CdiA-CT<sup>(M)</sup>/CdiI complex (Fig 7). On the other hand, CdiA-CT<sup>(M)</sup> has a  $T_m$  of  $55.2 \pm 0.2^\circ\text{C}$  and association of CysK to CdiA-CT<sup>(M)</sup> increases thermal stability by 10°C as CdiA-CT<sup>(M)</sup>/CysK complex has  $T_m$  of  $66.09 \pm 0.15^\circ\text{C}$ . Also, binding of CdiI stabilizes CdiA-CT<sup>(M)</sup> by ~4°C. This data suggests that CdiI binding stabilizes CdiA-CT<sup>(M)</sup> but CysK binding significantly enhances the thermal stability of both CdiA-CT<sup>(M)</sup> and CdiA-CT<sup>(M)</sup>/CdiI complex. The thermal stability results are in agreement with other CDI toxin/immunity

complexes from *E. coli* EC869 and *Burkholderia pseudomallei* 1026b where binding of immunity protein resulted in improved thermal stability of the toxin/immunity complexes [33].

## Discussion

CDI is an interesting mode of direct cell to cell communication in bacteria that provides a survival advantage to CDI<sup>+</sup> cells over CDI<sup>-</sup> cells. Pioneering work by Low's and Hayes's groups

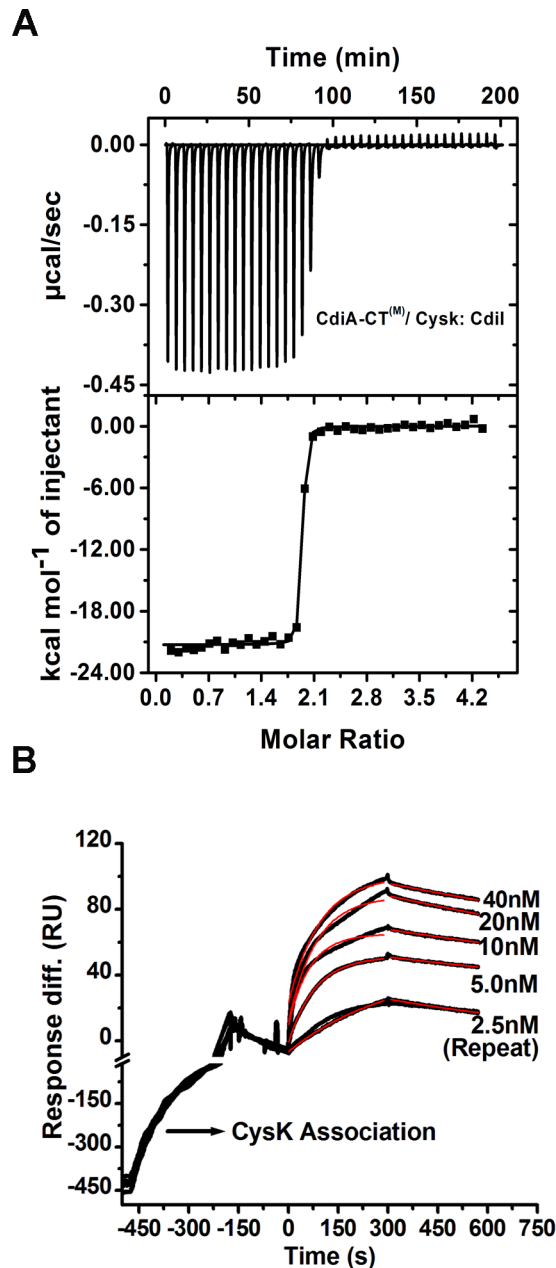


**Fig 5. Interactions of CdiA-CT/CysK and CdiI studied using ITC and SPR.** (A) ITC data suggests increased affinity of the CdiA-CT<sup>(M)</sup>/CysK complex for CdiI. (B) SPR data also suggests high affinity as a consequence of decreased dissociation rate. Both raw sensograms (black line) and fitted curves (red line) are shown in the figure. For better visualization of CysK/CdiA-CT<sup>(M)</sup> complex and CdiI interactions scale is broken at -10 RU on the y-axis and at -200 s on the x-axis. The CdiI association starts at 0 s and ends at 300 s followed by dissociation phase of 500 s but shown only up to 300 s.

doi:10.1371/journal.pone.0159844.g005

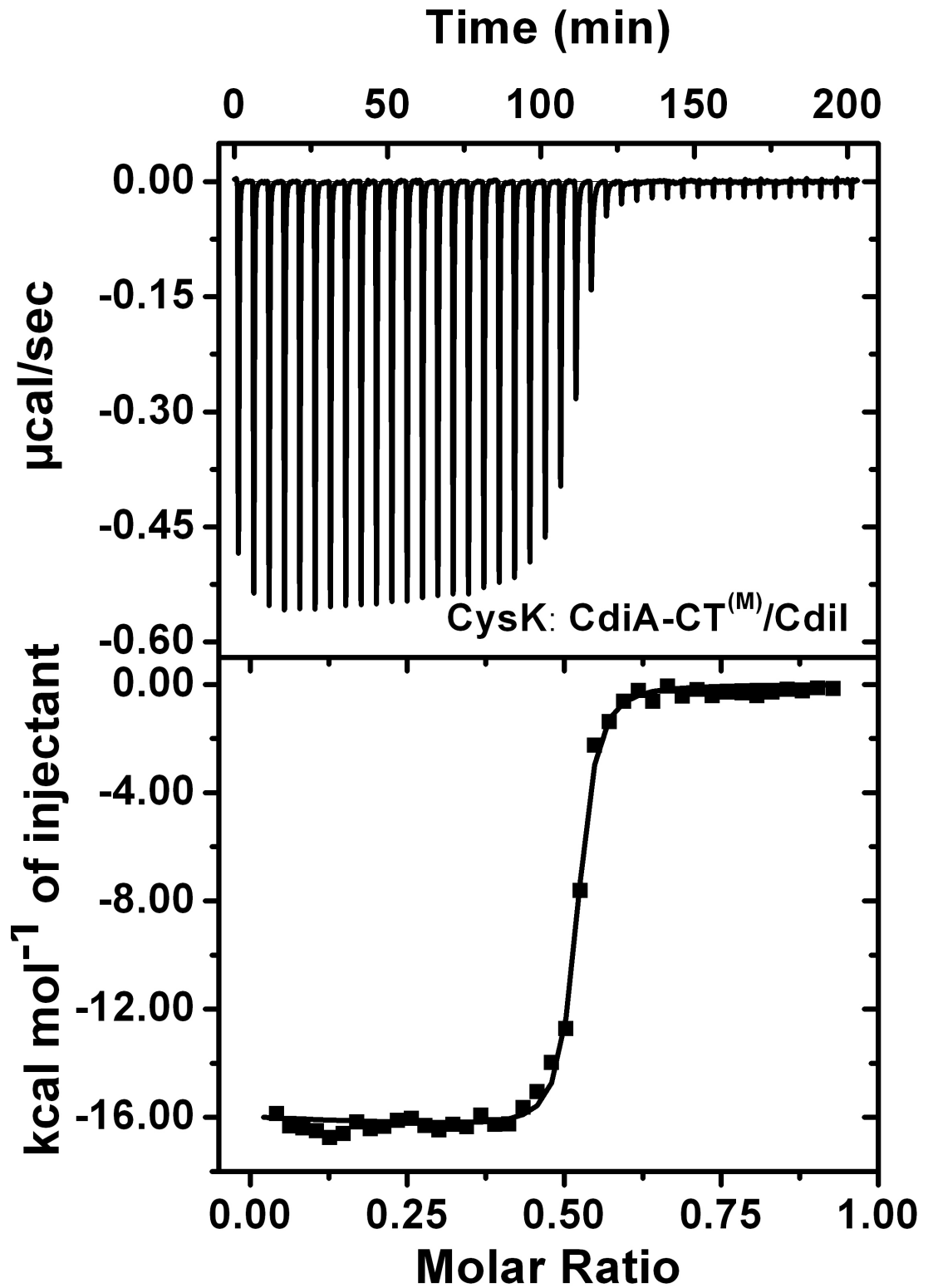


**Fig 6. Interactions of CdiA-CT<sup>(M)</sup>/CdiI and CysK studied using ITC.** ITC data suggests increased affinity of CysK for CdiA-CT<sup>(M)</sup>/CdiI complex.

doi:10.1371/journal.pone.0159844.g006

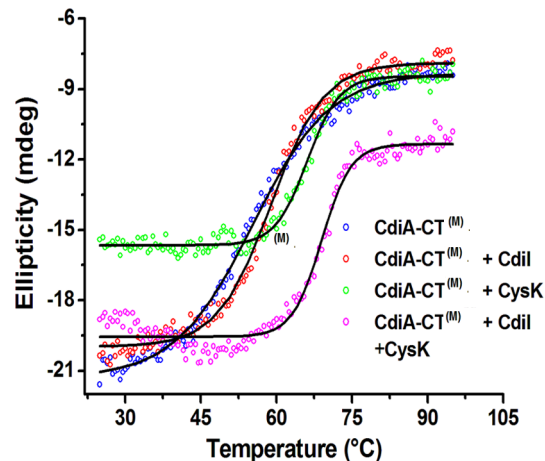


**Fig 7. Binding of CysK stabilizes the CdiA-CT<sup>(M)</sup>/CdiI complex.** Thermal stability of CdiA-CT<sup>(M)</sup> and other complexes was determined using CD melting studies. All the protein samples show two state melting curve. CysK stabilizes CdiA-CT<sup>(M)</sup> and CdiA-CT<sup>(M)</sup>/CdiI complex by ~10°C.

doi:10.1371/journal.pone.0159844.g007

has led to the discovery and detailed molecular dissection of the mechanism(s) involved in the CDI systems [7,9,11,21,24,34]. Body of the literature generated over a decade of research by these groups suggests that CDI involves several steps: i) expression of CdiA protein and its export to surface by CdiB in inhibitor cells, ii) cell to cell contact with the target cell, iii) receptor mediated CdiA-CT toxin uptake by target cell, iv) activation of the toxin in host by ‘cell permissive factor’ (optional step), v) target cell growth arrest, vi) protection of self by expression of immunity protein and hence promoting ‘self’ or ‘kin selection’. The presence of CdiA specific receptor protein on the target cell acts as a first line of the target selection [9,21]. Discovery of the role of CysK as a host ‘permissive factor’ has added one more distinguishing step to the existing complexity in the target selection in UPEC536 mediated CDI system. Based on the presence of conserved C-terminal isoleucine in many predicted CDI toxins, it has been proposed that host factor(s) may act as a second line of target selection [23,35]. However, it is intriguing why inhibitor cells chose conserved biosynthetic enzyme CysK as cell permissive factor which is also present in its own genetic makeup as well? Interestingly, CysK and CdiI bind simultaneously to CdiA-CT to form a stable inactive ternary complex in CDI<sup>+</sup> inhibitory cells [23]. Though ternary complex is inactive, the role of CysK in this ternary complex was not clear.

We used a combination of biophysical experiments to address this important question. In the CDI<sup>+</sup> inhibitory cell, the binding sequence of CdiI, CysK and CdiA-CT to form ternary complex is not defined. The ternary complex can be formed by two distinct sequence of interactions: 1) CdiI binding to the preformed CysK/CdiA-CT complex and 2) CysK binding to the preformed CdiA-CT/CdiI complex. We studied both possible binding sequence events. To our surprise, CysK bound CdiA-CT shows ~40 fold increased affinity for CdiI as compared to free CdiA-CT. This increase in stability is mainly due to ~130 fold reduction in dissociation rate. We propose that this reduced dissociation rate is beneficial for inhibitor cells as the ternary immunity complex captures the toxin in an inactive state for the extended period and hence offering better protection. Our data suggest, that UPEC536 cells adopted allosteric/inactivation strengthening mechanism, by increasing the affinity of toxin/immunity protein interactions upon binding of CysK, to neutralize toxic activity of CdiA-CT/CysK activated complex. In this mode of inhibition, CdiI might be exploiting conformational changes upon CysK binding as a selective pressure to preferably bind activated CdiA-CT/CysK complex and form a high affinity

inactive ternary complex with slower dissociation rate. Since CdiI dissociates rapidly from CdiA-CT/CdiI complex and dissociates at significantly much lower rate from the ternary complex hence, CdiI is engaged in preferably neutralizing active toxin/activator complex.

When we investigated the second binding sequence we observed that binding of CysK to preformed CdiA-CT /CdiI complex shows higher affinity as compared to CdiA-CT. These results suggest that CysK in CDI<sup>+</sup> inhibitor cells may preferably associate with CdiA-CT/CdiI complex than with toxin alone hence providing an additional survival benefit. Another similar interesting case of regulation of cysteine metabolism mediated by CysK/CymR interactions has been reported in *Bacillus subtilis*. CymR, master regulator of cysteine metabolism in *B. subtilis*, forms a stable complex with CysK. Binding of CysK to CymR increases the stability of CymR/*ytll* promoter DNA by ~7 fold mainly by reducing the dissociation rate, as inferred from the SPR studies [36]. CysK is conserved in bacteria and plants and is reportedly involved in several moonlighting functions where the interacting partner usually have conserved C-terminal isoleucine residue [35]. Though we have studied the role of CysK in UPEC536 strain but there are several toxin/immunity protein systems where the toxins have terminal Ile residue [35] so we believe CysK may play similar roles in those CDI modules as well. In future, it will be interesting to study binding kinetics of such systems as well. Thermal melting studies revealed that CysK binding also increases the thermal stability of the CdiA-CT and CdiA-CT/CdiI complex

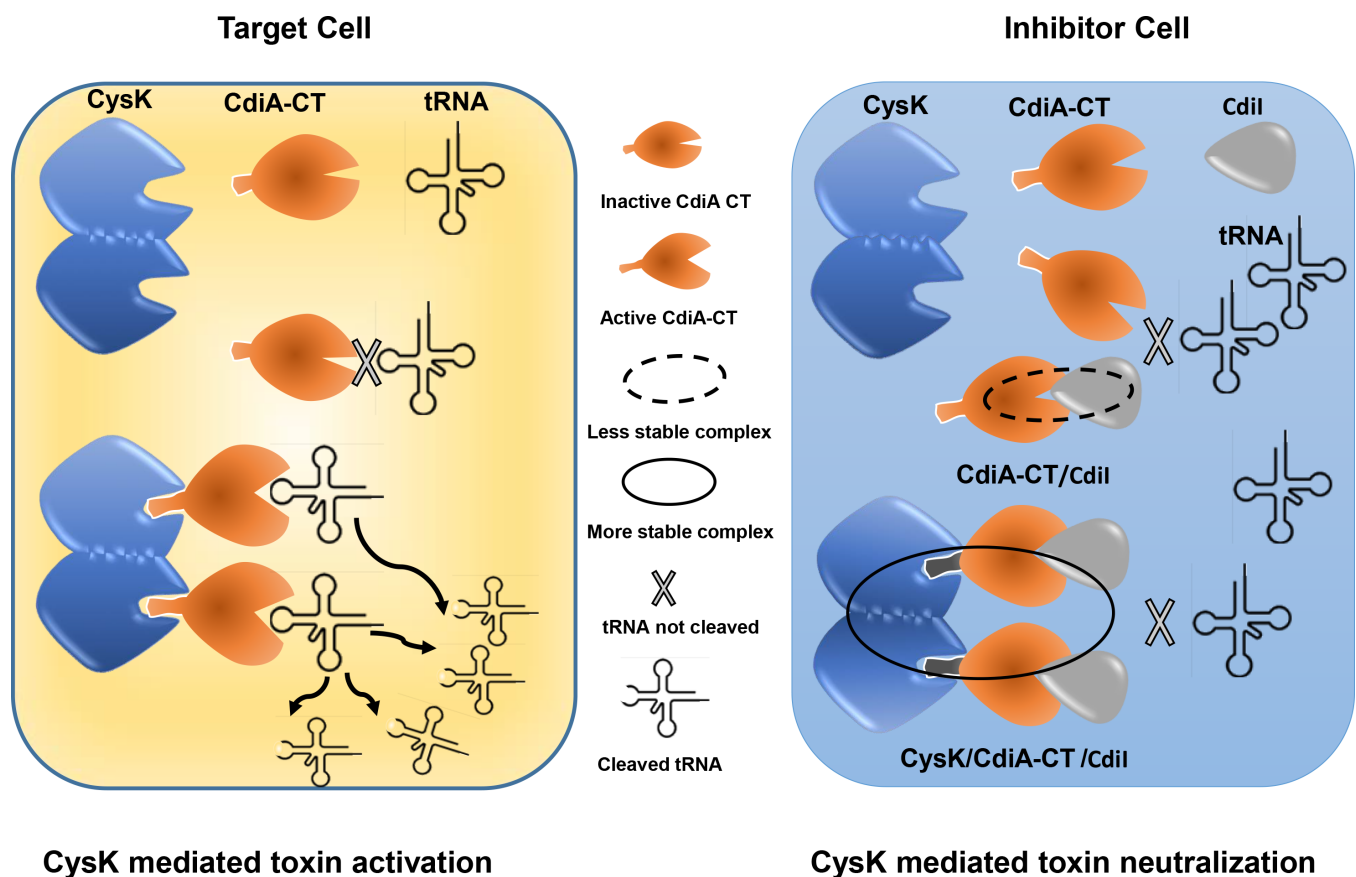


**Fig 8. Proposed model for the dual role of CysK in UPEC536 mediated CDI.** The left panel shows CysK mediated toxin activation in target cell where CysK dimer binds CdiA-CT and activates tRNAase activity causing growth arrest [23]. The right panel shows the moonlighting role of CysK as a modulator of CdiA-CT<sup>(M)</sup>/CdiI in the CDI<sup>+</sup> inhibitory cells, as proposed in the present study. Binding of CysK to CdiA-CT stabilizes CdiA-CT/CdiI immunity complex, primarily by decreasing dissociation rate, to prevent autoinhibition in UPEC536 inhibitor cells.

doi:10.1371/journal.pone.0159844.g008

by  $\sim 10^\circ\text{C}$ . So, CysK binding provides kinetic as well as thermal stability to the CdiA-CT/CdiI immunity complex.

We also studied stoichiometry and kinetics of CdiA-CT /CysK interactions as this complex is common in both target and inhibitor cells. CdiA-CT binds CysK with  $K_{D1}$  of  $79.3 \pm 8.9$  and  $K_{D2}$  of  $89.2 \pm 10.1$  nM and  $32 \pm 4$  nM as determined by ITC and SPR respectively. Interestingly, both  $k_{on}$  and  $k_{off}$  are significantly lower as compared to CdiA-CT/CdiI complex. Lower  $k_{off}$  is advantageous for the toxin as once activated, it may remain functional for a longer period, before the activated complex falls apart, causing prolonged damage to the target cell. AUC data suggests that CysK is predominantly dimer and CdiA-CT is predominantly monomer in solution. Based on the structural information available on close sequence homologs of CysK, the two CdiA-CT binding sites are positioned on the same face of the CysK dimer [37]. So, either two molecules of CdiA-CT can bind CysK dimer or binding of one CdiA-CT molecule may sterically occlude binding of the other molecule. To check stoichiometry of the complex we performed AUC experiments which suggest that CysK and CdiA-CT associate to form 2:2 stoichiometric heterotetramer in solution. Though the mechanism of the toxin activation is not yet clear, but based on the data presented here we speculate that CysK brings two molecules of CdiA-CT in close proximity and along with subtle conformational rearrangements may activate CdiA-CT.

To summarize, this study demonstrates a distinct function of CysK in UPEC536 cells. We propose that CdiA-CT/CysK interactions, besides toxin activation, might have also evolved to enhance inherently weaker CdiA-CT/CdiI interactions to ensure better survival of inhibitor cells upon entry of CdiA-CT from the neighbouring CDI<sup>+</sup> UPEC536 cells (Fig 8). This discovery adds one more role to the growing list of moonlighting functions mediated by CysK [35,36,38]. In future, more detailed structural/biophysical studies are needed to unravel the mechanism by which CysK or similar moonlighting proteins enhance the stability of protein-protein or protein-DNA complexes to perform some important biological functions.

## Acknowledgments

KGT and SK would like to thank Dr. S. Kumaran and Gundeep Kaur CSIR-IMTECH for their valuable feedback on AUC data analysis. KGT thanks Structural Genomics Consortium, Karolinska Institute, Stockholm, Sweden for kind gift of pNIC28-Bsa4. We thank anonymous reviewers for their constructive criticism and insightful suggestions.

## Author Contributions

Conceived and designed the experiments: KGT SK. Performed the experiments: SK MU. Analyzed the data: SK KGT. Wrote the paper: KGT SK.

## References

1. Keller L, Surette MG (2006) Communication in bacteria: an ecological and evolutionary perspective. *Nat Rev Microbiol* 4: 249–258. PMID: [16501584](#)
2. Bassler BL, Losick R (2006) Bacterially speaking. *Cell* 125: 237–246. PMID: [16630813](#)
3. Dunny GM, Brickman TJ, Dworkin M (2008) Multicellular behavior in bacteria: communication, cooperation, competition and cheating. *Bioessays* 30: 296–298. doi: [10.1002/bies.20740](#) PMID: [18348154](#)
4. Miller MB, Bassler BL (2001) Quorum sensing in bacteria. *Annu Rev Microbiol* 55: 165–199. PMID: [11544353](#)
5. Zhang D, Iyer LM, Aravind L (2011) A novel immunity system for bacterial nucleic acid degrading toxins and its recruitment in various eukaryotic and DNA viral systems. *Nucleic Acids Res* 39: 4532–4552. doi: [10.1093/nar/gkr036](#) PMID: [21306995](#)



6. Bassler BL (1999) How bacteria talk to each other: regulation of gene expression by quorum sensing. *Curr Opin Microbiol* 2: 582–587. PMID: [10607620](#)
7. Aoki SK, Pamma R, Hernday AD, Bickham JE, Braaten BA, et al. (2005) Contact-dependent inhibition of growth in *Escherichia coli*. *Science* 309: 1245–1248. PMID: [16109881](#)
8. Tommassen J (2007) Getting into and through the outer membrane. *Science* 317: 903–904. PMID: [17702930](#)
9. Aoki SK, Malinverni JC, Jacoby K, Thomas B, Pamma R, et al. (2008) Contact-dependent growth inhibition requires the essential outer membrane protein BamA (YaeT) as the receptor and the inner membrane transport protein AcrB. *Mol Microbiol* 70: 323–340. doi: [10.1111/j.1365-2958.2008.06404.x](#) PMID: [18761695](#)
10. Aoki SK, Poole SJ, Hayes CS, Low DA (2011) Toxin on a stick: modular CDI toxin delivery systems play roles in bacterial competition. *Virulence* 2: 356–359. PMID: [21705856](#)
11. Aoki SK, Diner EJ, de Roodenbeke CT, Burgess BR, Poole SJ, et al. (2010) A widespread family of polymorphic contact-dependent toxin delivery systems in bacteria. *Nature* 468: 439–442. doi: [10.1038/nature09490](#) PMID: [21085179](#)
12. Jacob-Dubuisson F, Fernandez R, Coutte L (2004) Protein secretion through autotransporter and two-partner pathways. *Biochimica Et Biophysica Acta-Molecular Cell Research* 1694: 235–257.
13. Zhang D, de Souza RF, Anantharaman V, Iyer LM, Aravind L (2012) Polymorphic toxin systems: Comprehensive characterization of trafficking modes, processing, mechanisms of action, immunity and ecology using comparative genomics. *Biol Direct* 7: 18. doi: [10.1186/1745-6150-7-18](#) PMID: [22731697](#)
14. Anderson MS, Garcia EC, Cotter PA (2012) The Burkholderia bcpAIOB genes define unique classes of two-partner secretion and contact dependent growth inhibition systems. *PLoS Genet* 8: e1002877. doi: [10.1371/journal.pgen.1002877](#) PMID: [22912595](#)
15. Nikolakakis K, Amber S, Wilbur JS, Diner EJ, Aoki SK, et al. (2012) The toxin/immunity network of *Burkholderia pseudomallei* contact-dependent growth inhibition (CDI) systems. *Mol Microbiol* 84: 516–529. doi: [10.1111/j.1365-2958.2012.08039.x](#) PMID: [22435733](#)
16. Hayes CS, Koskiniemi S, Ruhe ZC, Poole SJ, Low DA (2014) Mechanisms and biological roles of contact-dependent growth inhibition systems. *Cold Spring Harb Perspect Med* 4.
17. Anderson MS, Garcia EC, Cotter PA (2014) Kind discrimination and competitive exclusion mediated by contact-dependent growth inhibition systems shape biofilm community structure. *PLoS Pathog* 10: e1004076. doi: [10.1371/journal.ppat.1004076](#) PMID: [24743836](#)
18. Garcia EC, Anderson MS, Hagar JA, Cotter PA (2013) *Burkholderia* BcpA mediates biofilm formation independently of interbacterial contact-dependent growth inhibition. *Mol Microbiol* 89: 1213–1225. doi: [10.1111/mmi.12339](#) PMID: [23879629](#)
19. Foxman B (2003) Epidemiology of urinary tract infections: incidence, morbidity, and economic costs. *Dis Mon* 49: 53–70. PMID: [12601337](#)
20. Webb JS, Nikolakakis KC, Willett JLE, Aoki SK, Hayes CS, et al. (2013) Delivery of CdiA Nuclease Toxins into Target Cells during Contact-Dependent Growth Inhibition. *Plos One* 8.
21. Beck CM, Diner EJ, Kim JJ, Low DA, Hayes CS (2014) The F pilus mediates a novel pathway of CDI toxin import. *Mol Microbiol* 93: 276–290. doi: [10.1111/mmi.12658](#) PMID: [24889811](#)
22. Willett JL, Gucinski GC, Fatherree JP, Low DA, Hayes CS (2015) Contact-dependent growth inhibition toxins exploit multiple independent cell-entry pathways. *Proc Natl Acad Sci U S A* 112: 11341–11346. doi: [10.1073/pnas.1512124112](#) PMID: [26305955](#)
23. Diner EJ, Beck CM, Webb JS, Low DA, Hayes CS (2012) Identification of a target cell permissive factor required for contact-dependent growth inhibition (CDI). *Genes Dev* 26: 515–525. doi: [10.1101/gad.182345.111](#) PMID: [22333533](#)
24. Poole SJ, Diner EJ, Aoki SK, Braaten BA, t'Kint de Roodenbeke C, et al. (2011) Identification of functional toxin/immunity genes linked to contact-dependent growth inhibition (CDI) and rearrangement hot-spot (Rhs) systems. *PLoS Genet* 7: e1002217. doi: [10.1371/journal.pgen.1002217](#) PMID: [21829394](#)
25. Schuck P, Perugini MA, Gonzales NR, Howlett GJ, Schubert D (2002) Size-distribution analysis of proteins by analytical ultracentrifugation: strategies and application to model systems. *Biophys J* 82: 1096–1111. PMID: [11806949](#)
26. Laue TM, Shah BD., Ridgeway TM., Pelletier SL (1992) Computer-aided interpretation of analytical sedimentation data for proteins. In: Harding AJRaJCH S. E., editor. *Analytical Ultracentrifugation in Biochemistry and Polymer Science*. Horton. Cambridge,; Royal Society of Chemistry. pp. 90–25.
27. Francois JA, Kumaran S, Jez JM (2006) Structural basis for interaction of O-acetylserine sulfhydrylase and serine acetyltransferase in the Arabidopsis cysteine synthase complex. *Plant Cell* 18: 3647–3655. PMID: [17194764](#)

28. Kumaran S, Jez JM (2007) Thermodynamics of the interaction between O-Acetylserine sulfhydrylase and the C-terminus of serine acetyltransferase. *Biochemistry* 46: 5586–5594. PMID: [17425333](#)
29. Ghafourian S, Raftari M, Sadeghifard N, Sekawi Z (2014) Toxin-antitoxin Systems: Classification, Biological Function and Application in Biotechnology. *Curr Issues Mol Biol* 16: 9–14. PMID: [23652423](#)
30. Overgaard M, Borch J, Gerdes K (2009) RelB and RelE of *Escherichia coli* form a tight complex that represses transcription via the ribbon-helix-helix motif in RelB. *J Mol Biol* 394: 183–196. doi: [10.1016/j.jmb.2009.09.006](#) PMID: [19747491](#)
31. Florek P, Levnikov VM, Blagova E, Lebedev AA, Skrabana R, et al. (2011) The structure and interactions of SpoIIISA and SpoII SB, a toxin-antitoxin system in *Bacillus subtilis*. *J Biol Chem* 286: 6808–6819. doi: [10.1074/jbc.M110.172429](#) PMID: [21147767](#)
32. Heaton BE, Herrou J, Blackwell AE, Wysocki VH, Crosson S (2012) Molecular structure and function of the novel BrnT/BrnA toxin-antitoxin system of *Brucella abortus*. *J Biol Chem* 287: 12098–12110. doi: [10.1074/jbc.M111.332163](#) PMID: [22334680](#)
33. Yamamoto K, Oshima T, Nonaka G, Ito H, Ishihama A (2011) Induction of the *Escherichia coli* cysK gene by genetic and environmental factors. *FEMS Microbiol Lett* 323: 88–95. doi: [10.1111/j.1574-6968.2011.02364.x](#) PMID: [22092684](#)
34. Ruhe ZC, Wallace AB, Low DA, Hayes CS (2013) Receptor polymorphism restricts contact-dependent growth inhibition to members of the same species. *MBio* 4.
35. Campanini B, Benoni R, Bettati S, Beck CM, Hayes CS, et al. (2015) Moonlighting O-acetylserine sulfhydrylase: New functions for an old protein. *Biochim Biophys Acta* 1854: 1184–1193. doi: [10.1016/j.bbapap.2015.02.013](#) PMID: [25731080](#)
36. Tanous C, Soutourina O, Raynal B, Hullo MF, Mervelet P, et al. (2008) The CymR regulator in complex with the enzyme CysK controls cysteine metabolism in *Bacillus subtilis*. *J Biol Chem* 283: 35551–35560. doi: [10.1074/jbc.M805951200](#) PMID: [18974048](#)
37. Rabeh WM, Cook PF (2004) Structure and mechanism of O-acetylserine sulfhydrylase. *J Biol Chem* 279: 26803–26806. PMID: [15073190](#)
38. Jeffery CJ (1999) Moonlighting proteins. *Trends Biochem Sci* 24: 8–11. PMID: [10087914](#)